

# MeLSI: Metric Learning for Statistical Inference in Microbiome Community Composition Analysis

Nathan Bresette<sup>1</sup>, Aaron Ericsson<sup>2</sup>, Carter Woods<sup>3</sup>, Ai-Ling Lin<sup>4</sup>

<sup>1</sup> [Affiliation to be added]

<sup>2</sup> [Affiliation to be added]

<sup>3</sup> [Affiliation to be added]

<sup>4</sup> [Affiliation to be added]

---

## Abstract

Microbiome beta diversity analysis relies on distance-based methods including PERMANOVA combined with fixed ecological distance metrics (Bray-Curtis, Euclidean, Jaccard, and UniFrac), which treat all microbial taxa uniformly regardless of their biological relevance to community differences. This “one-size-fits-all” approach may miss subtle but biologically meaningful patterns in complex microbiome data. We present MeLSI (Metric Learning for Statistical Inference), a novel machine learning framework that learns data-adaptive distance metrics optimized for detecting community composition differences in multivariate microbiome analyses. MeLSI employs an ensemble of weak learners using bootstrap sampling, feature subsampling, and gradient-based optimization to learn optimal feature weights, combined with rigorous permutation testing for statistical inference. The learned metrics can be used with PERMANOVA for hypothesis testing and with Principal Coordinates Analysis (PCoA) for ordination visualization. Comprehensive validation on synthetic benchmarks and real datasets shows that MeLSI maintains proper Type I error control while delivering competitive or superior F-statistics when signal structure aligns with CLR-based weighting and, crucially, supplies interpretable feature-weight profiles that clarify which taxa drive group separation. On the Atlas1006 dataset, MeLSI achieved stronger effect sizes than the best traditional methods, and even when performance was comparable, the learned feature weights provided biological insight that fixed metrics cannot supply. MeLSI therefore offers a statistically rigorous tool that augments beta diversity analysis with transparent, data-driven interpretability.

**Keywords:** microbiome analysis, metric learning, beta diversity, community composition, PERMANOVA, distance metrics, permutation testing

---

## 1. Introduction

### 1.1 The Microbiome and Human Health

The human microbiome, the complex community of microorganisms inhabiting our bodies, plays fundamental roles in health and disease (Gilbert et al., 2018; Shreiner et al., 2015). Recent advances in high-throughput sequencing technologies have enabled comprehensive profiling of microbial communities, revealing associations between microbiome composition and diverse conditions including inflammatory bowel disease, obesity, diabetes, and neurological disorders (Lynch & Pedersen, 2016; Clemente et al., 2012). A central question in microbiome research is comparing overall microbial community composition between groups (e.g., healthy vs. diseased individuals), typically assessed through beta diversity analysis, which studies compositional differences between samples.

### 1.2 Current Approaches and Their Limitations

Microbiome beta diversity analysis predominantly relies on distance-based multivariate methods including PERMANOVA (Permutational Multivariate Analysis of Variance) combined with fixed ecological distance metrics (Anderson, 2017; McArdle & Anderson, 2001). Commonly used metrics include Bray-Curtis dissimilarity, Euclidean distance, Jaccard index, and phylogenetically-informed metrics including UniFrac (Lozupone & Knight, 2005). These approaches have proven valuable for hypothesis testing about community differences and visualization through ordination methods like Principal Coordinates Analysis (PCoA) (Ramette, 2007).

However, fixed distance metrics suffer from a fundamental limitation. They apply the same mathematical formula to all datasets, treating all microbial taxa with equal importance regardless of their biological relevance to the specific research question (Knights et al., 2011). For instance, Bray-Curtis dissimilarity equally weights all taxa based on their relative abundances, while Euclidean distance treats all features identically. This “one-size-fits-all” approach may fail to capture subtle but biologically meaningful differences when only a subset of taxa drive group separation (Weiss et al., 2017).

Furthermore, microbiome data presents unique analytical challenges including high dimensionality (often hundreds to thousands of taxa), compositionality (relative abundances sum to a constant), sparsity (many zero counts), and heterogeneous biological signal across features (Gloor et al., 2017). Fixed metrics cannot adapt to these complexities in a data-driven manner.

### 1.3 The Need for Statistical Rigor

A critical requirement for any beta diversity method is proper statistical inference with controlled Type I error rates (false positive rates). While machine learning approaches often prioritize predictive accuracy, hypothesis testing for

community composition differences requires rigorous F-statistic and p-value calculation under the null hypothesis of no group differences (Westfall & Young, 1993). Permutation testing provides a non-parametric framework for valid inference that makes minimal distributional assumptions (Good, 2013), making it particularly suitable for complex microbiome data and distance-based analyses like PERMANOVA.

#### 1.4 Metric Learning: An Emerging Paradigm

Metric learning, a branch of machine learning, offers a principled approach to address these limitations (Kulis, 2013; Bellet et al., 2013). Rather than using fixed distance formulas, metric learning algorithms learn optimal distance metrics from data by identifying which features contribute most to separating groups of interest. In the context of supervised learning, metric learning algorithms optimize distance functions to maximize between-group distances while minimizing within-group distances (Weinberger & Saul, 2009; Xing et al., 2002).

Mahalanobis distance learning (Mahalanobis, 1936) learns a positive semi-definite matrix  $\mathbf{M}$  that defines distances as  $d(\mathbf{x}_i, \mathbf{x}_j) = \sqrt{(\mathbf{x}_i - \mathbf{x}_j)^T \mathbf{M} (\mathbf{x}_i - \mathbf{x}_j)}$ . When  $\mathbf{M}$  is diagonal, this reduces to learning feature-specific weights, providing interpretable importance scores (Xing et al., 2002).

Despite its promise, metric learning has seen limited application in microbiome beta diversity analysis. Previous work has explored metric learning for clinical prediction tasks (Pasolli et al., 2016), but not specifically for statistical inference in community composition analysis where rigorous Type I error control is essential.

#### 1.5 Study Objectives

We developed MeLSI (Metric Learning for Statistical Inference) to bridge the gap between adaptive machine learning approaches and rigorous statistical inference for microbiome beta diversity and community composition analysis. Our specific objectives were to (1) design an ensemble metric learning framework that learns data-adaptive distance metrics for PERMANOVA and ordination while preventing overfitting, (2) integrate metric learning with permutation testing to ensure valid statistical inference, (3) comprehensively validate Type I error control, statistical power, scalability, parameter sensitivity, and computational efficiency, (4) demonstrate practical utility on real microbiome datasets, and (5) provide interpretable feature importance scores to identify biologically relevant taxa driving community separation.

This paper presents the MeLSI framework, comprehensive validation results, and discussion of its implications for microbiome beta diversity research.

---

## 2. Methods

### 2.1 Overview of the MeLSI Framework

MeLSI integrates metric learning with permutation-based statistical inference through three main phases:

#### Phase 1: Metric Learning

1. Apply conservative pre-filtering to focus on high-variance features
2. For each of  $B$  weak learners:
  - Bootstrap sample the data
  - Subsample features
  - Optimize metric matrix  $\mathbf{M}$  via gradient descent
3. Combine weak learners via performance-weighted ensemble averaging
4. Compute robust distance matrix using eigenvalue decomposition

#### Phase 2: Statistical Inference

5. Calculate observed F-statistic using the learned metric
6. Generate null distribution via permutation testing (relearn metric on each permutation)
7. Compute permutation-based p-value

Each component addresses specific challenges in microbiome data analysis while maintaining statistical validity. The following sections formalize the mathematical framework and detail each algorithmic component, organized by phase.

### 2.2 Phase 1: Metric Learning

**2.2.1 Problem Formulation** Let  $\mathbf{X} \in \mathbb{R}^{n \times p}$  denote a feature abundance matrix with  $n$  samples and  $p$  taxa (features), and let  $\mathbf{y} = (y_1, \dots, y_n)$  denote group labels. Our goal is to learn a distance metric optimized for separating groups defined by  $\mathbf{y}$  while ensuring valid statistical inference.

We parameterize the distance metric using a diagonal positive semi-definite matrix  $\mathbf{M} \in \mathbb{R}^{p \times p}$ , where  $M_{jj}$  represents the weight (importance) of feature  $j$ . The learned Mahalanobis distance between samples  $i$  and  $k$  is:

$$d_M(\mathbf{x}_i, \mathbf{x}_k) = \sqrt{(\mathbf{x}_i - \mathbf{x}_k)^T \mathbf{M} (\mathbf{x}_i - \mathbf{x}_k)}$$

For diagonal  $\mathbf{M}$ , this simplifies to a weighted Euclidean distance:

$$d_M(\mathbf{x}_i, \mathbf{x}_k) = \sqrt{\sum_j M_{jj} (x_{ij} - x_{kj})^2}$$

**2.2.2 Conservative Pre-filtering** To improve computational efficiency and reduce noise, MeLSI applies conservative variance-based pre-filtering. For pairwise comparisons, we calculate a feature importance score combining mean differences and variance:

$$I_j = \frac{|\mu_{1j} - \mu_{2j}|}{\sqrt{\sigma_{1j}^2 + \sigma_{2j}^2}}$$

where  $\mu_{1j}$  and  $\mu_{2j}$  are the mean abundances of feature  $j$  in groups 1 and 2, and  $\sigma_{1j}^2$  and  $\sigma_{2j}^2$  are their variances. We retain the top 70% of features by this importance score, maintaining high statistical power while reducing dimensionality.

For multi-group comparisons (3 or more groups), we use ANOVA F-statistics to rank features and apply the same 70% retention threshold. Critically, this pre-filtering is applied consistently to both observed and permuted data during null distribution generation to avoid bias.

**2.2.3 Ensemble Learning with Weak Learners** MeLSI constructs an ensemble of  $B$  weak learners (default  $B = 30$ ) to improve robustness and prevent overfitting. For each weak learner  $b$ :

1. **Bootstrap sampling:** Draw  $n$  samples with replacement from the original data to create a bootstrap dataset  $(\mathbf{X}_b, \mathbf{y}_b)$
2. **Feature subsampling:** Randomly select  $m = \lfloor p \times m_{frac} \rfloor$  features (default  $m_{frac} = 0.8$ ) without replacement
3. **Metric optimization:** Learn  $\mathbf{M}_b$  on the bootstrapped, subsampled data

The combination of bootstrap sampling (sample-level randomness) and feature subsampling (feature-level randomness) ensures diversity among weak learners, reducing overfitting risk (Breiman, 2001).

**2.2.4 Optimization Objective** For each weak learner, we optimize  $\mathbf{M}$  to maximize between-group distances while minimizing within-group distances. For a two-group comparison (groups  $G_1$  and  $G_2$ ), we maximize the objective:

$$F(\mathbf{M}) = \frac{1}{|G_1||G_2|} \sum_{i \in G_1} \sum_{k \in G_2} d_M(\mathbf{x}_i, \mathbf{x}_k)^2 - \frac{1}{2|G_1|^2} \sum_{i,j \in G_1} d_M(\mathbf{x}_i, \mathbf{x}_j)^2 - \frac{1}{2|G_2|^2} \sum_{i,j \in G_2} d_M(\mathbf{x}_i, \mathbf{x}_j)^2$$

This objective encourages large between-group distances and small within-group distances, analogous to maximizing the F-ratio in ANOVA. This formulation is inspired by standard metric learning objectives that maximize between-class to within-class distance ratios (Xing et al., 2002; Weinberger & Saul, 2009), adapted here for direct compatibility with PERMANOVA’s F-statistic framework.

**2.2.5 Gradient-Based Optimization** Each weak learner optimizes its metric matrix  $\mathbf{M}$  using stochastic gradient descent. At each iteration  $t$ :

1. Sample one within-group pair from each group:  $(i_1, j_1)$  from  $G_1$ ,  $(i_2, j_2)$  from  $G_2$
2. Sample one between-group pair:  $(i_1, i_2)$  where  $i_1 \in G_1$ ,  $i_2 \in G_2$
3. Compute gradient components:
  - Between-group gradient:  $\nabla_{between} = (\mathbf{x}_{i_1} - \mathbf{x}_{i_2})^2$
  - Within-group gradient:  $\nabla_{within} = -[(\mathbf{x}_{i_1} - \mathbf{x}_{j_1})^2 + (\mathbf{x}_{i_2} - \mathbf{x}_{j_2})^2]/2$
4. Update diagonal elements:  $M_{jj}^{(t+1)} = M_{jj}^t + \eta_t(\nabla_{between} + \nabla_{within})_j$

where  $\eta_t = \eta_0/(1 + 0.1t)$  is an adaptive learning rate (default  $\eta_0 = 0.1$ ). We constrain  $M_{jj} \geq 0.01$  to ensure positive definiteness and prevent numerical instability.

Early stopping is implemented by monitoring F-statistics every 20 iterations. If performance stagnates (no improvement for 5 consecutive checks), optimization terminates to prevent overfitting.

**2.2.6 Ensemble Averaging with Performance Weighting** After training all weak learners, we combine them into a final ensemble metric  $\mathbf{M}_{ensemble}$  using performance-weighted averaging:

$$\mathbf{M}_{ensemble} = \sum_b w_b \mathbf{M}_b$$

where weights are normalized F-statistics:

$$w_b = \frac{F_b}{\sum_{b'} F_{b'}}$$

and  $F_b$  is the PERMANOVA F-statistic achieved by weak learner  $b$  on its bootstrap sample. This weighting scheme emphasizes better-performing learners while maintaining diversity.

**2.2.7 Robust Distance Calculation** To ensure numerical stability, we compute the learned Mahalanobis distance using eigenvalue decomposition:

1. Compute eigendecomposition:  $\mathbf{M}_{ensemble} = \mathbf{V}\Lambda\mathbf{V}^T$  where  $\mathbf{V}$  is the matrix of eigenvectors and  $\Lambda$  is the diagonal matrix of eigenvalues
2. Enforce positive eigenvalues:  $\Lambda_{ii} \leftarrow \max(\Lambda_{ii}, 10^{-6})$
3. Compute  $\mathbf{M}^{-1/2} = \mathbf{V}\Lambda^{-1/2}\mathbf{V}^T$
4. Transform data:  $\mathbf{Y} = \mathbf{X}\mathbf{M}^{-1/2}$
5. Calculate Euclidean distances in transformed space:  $d_M = \|\mathbf{y}_i - \mathbf{y}_k\|_2$

This approach is more numerically stable than direct matrix inversion, particularly for high-dimensional data.

## 2.3 Phase 2: Statistical Inference

**2.3.1 Test Statistic** We use the PERMANOVA F-statistic as our test statistic (Anderson, 2017):

$$F_{obs} = \frac{SS_{between}/(k - 1)}{SS_{within}/(n - k)}$$

where  $SS_{between}$  is the between-group sum of squares,  $SS_{within}$  is the within-group sum of squares,  $k$  is the number of groups, and  $n$  is the total number of samples. This statistic measures how well the learned metric separates groups relative to within-group variation.

**2.3.2 Null Distribution Generation** To compute valid p-values, we generate a null distribution under the hypothesis of no group differences:

1. Permute group labels:  $\mathbf{y}_{perm} \leftarrow$  random permutation of  $\mathbf{y}$
2. Apply identical pre-filtering to permuted data
3. Learn metric  $\mathbf{M}_{perm}$  on  $(\mathbf{X}_{filtered}, \mathbf{y}_{perm})$  using the full MeLSI algorithm (repeating Phase 1: pre-filtering, ensemble construction, and metric optimization)
4. Calculate  $F_{perm}$  on  $(\mathbf{X}_{filtered}, \mathbf{y}_{perm})$  with  $\mathbf{M}_{perm}$
5. Repeat steps 1-4 for  $n_{perms}$  permutations (default  $n_{perms} = 200$ )

This approach ensures that the null distribution accurately reflects the variability introduced by the metric learning procedure itself, avoiding anticonservative (inflated Type I error) inference.

**2.3.3 P-value Calculation** The permutation-based p-value is computed as:

$$p = \frac{\sum \mathbb{I}(F_{perm} \geq F_{obs}) + 1}{n_{perms} + 1}$$

where  $\mathbb{I}$  is the indicator function. The “+1” terms provide a small-sample correction ensuring  $p \geq 1/(n_{perms} + 1)$  (Phipson & Smyth, 2010).

## 2.4 Multi-Group Extensions

**2.4.1 Omnibus Analysis** For studies with three or more groups, MeLSI provides an omnibus test that jointly evaluates differences across all groups. The optimization objective is modified to randomly sample group pairs at each gradient iteration, ensuring the learned metric captures global patterns rather than focusing on specific pairwise comparisons.

**2.4.2 Post-hoc Pairwise Comparisons** When the omnibus test is significant, MeLSI performs all pairwise comparisons, learning comparison-specific metrics for each pair. P-values are adjusted for multiple testing using the Benjamini-Hochberg false discovery rate (FDR) procedure (Benjamini & Hochberg, 1995).

## 2.5 Implementation and Computational Considerations

MeLSI is implemented in R (version  $\geq 4.0$ ) as an open-source package. Key dependencies include `vegan` (Oksanen et al., 2020) for PERMANOVA calculations, `ggplot2` (Wickham, 2016) for visualization, and base R for matrix operations. The algorithm is parallelizable across permutations and weak learners, though the current implementation is serial.

Time complexity is  $O(n^2 p^2 B \cdot n\_perms)$  in the worst case, but conservative pre-filtering reduces effective dimensionality, and early stopping in gradient descent reduces iteration counts. For typical microbiome datasets ( $n < 500$ ,  $p < 1000$ ), analysis completes in minutes on standard hardware.

## 2.6 Validation Experiments

We conducted comprehensive validation experiments to assess:

1. **Type I error control and statistical power:** Performance on null data (no true group differences) and ability to detect true effects of varying magnitude across synthetic and real datasets (Sections 3.1-3.2)
2. **Comparative performance on real datasets:** Validation against standard distance metrics on Atlas1006 and DietSwap datasets (Section 3.2)
3. **Scalability:** Performance across varying sample sizes and dimensionalities (Section 3.3)
4. **Parameter sensitivity:** Robustness to hyperparameter choices (Section 3.4)
5. **Pre-filtering value:** Benefit of conservative feature pre-filtering (Section 3.5)
6. **Biological interpretability:** Feature importance weights and visualization (Section 3.6)
7. **Computational performance:** Runtime characteristics on standard hardware (Section 3.7)

**2.6.1 Synthetic Data Generation** Synthetic datasets were generated using negative binomial count distributions to mimic microbiome abundance profiles. For each experiment we drew counts as  $X_{ij} \sim NB(\mu = 30, \text{size} = 0.8)$  and set values smaller than three to zero to induce sparsity. Unless otherwise noted, we simulated  $n = 100$  samples and  $p = 200$  taxa split evenly across two groups. To introduce signal we multiplied a subset of taxa in the first group by fold changes of 1.5 (5 taxa, “small” effect), 2.0 (10 taxa, “medium” effect), or 3.0 (20 taxa, “large” effect). Sample size ( $n$ ) and dimensionality ( $p$ ) were varied

in the scalability experiments (Section 3.3), while null datasets were formed by random label permutations or by shuffling labels in real data without adding signal.

### 2.6.2 Real Data Sources

Real microbiome datasets included:

1. **Atlas1006** (Lahti et al., 2014): 1,114 Western European adults with 123 genus-level taxa from HITChip microarray technology. Analysis compared males (n=560) versus females (n=554).
2. **DietSwap** (O’Keefe et al., 2015): 74 stool samples from African American adults participating in a short-term dietary intervention. We analyzed the timepoint-within-group baseline samples (timepoint.within.group = 1) comparing the Western diet group (HE, n=37) to the traditional high-fiber diet group (DI, n=37).

Data were preprocessed using centered log-ratio (CLR) transformation for Euclidean distance analyses to address compositionality (Aitchison, 1986; Gloor et al., 2017). Bray-Curtis dissimilarity, Jaccard, and UniFrac distances were computed on raw count data, as these metrics are inherently designed to handle compositional data (Legendre & Gallagher, 2001; Lozupone & Knight, 2005).

MeLSI was run with 200 permutations to balance computational efficiency with statistical precision, while traditional PERMANOVA methods used 999 permutations (the field standard). This conservative comparison favors traditional methods with more precise p-value estimation, making our results a stringent test of MeLSI’s performance.

**2.6.3 Comparison Methods** MeLSI was compared against standard PERMANOVA analyses using five fixed distance metrics: Bray-Curtis dissimilarity, Euclidean distance, Jaccard dissimilarity, weighted UniFrac (phylogenetic, where applicable), and unweighted UniFrac (phylogenetic, where applicable).

---

## 3. Results

### 3.1 Type I Error Control

Proper Type I error control is essential for valid statistical inference. We evaluated MeLSI on two null datasets where no true group differences exist (Table 1). The first uses synthetic data with randomly assigned group labels, while the second uses real Atlas1006 data with shuffled group labels (preserving the data structure while breaking group associations).

**Table 1. Type I Error Control on Null Data**

Dataset	n	p	F	MeLSI	MeLSI	Best Traditional	Best Trad F	Best Trad p
Null Synthetic	200	200	1.307	0.607		Euclidean	0.964	0.638
Null Real Shuffled	200	130	1.737	0.224		Euclidean	1.215	0.249

On synthetic null data (randomly assigned group labels), MeLSI achieved  $F = 1.307$  with  $p = 0.607$ , indicating no false positive signal. Traditional methods also maintained proper Type I error control, with Euclidean ( $F = 0.964$ ,  $p = 0.638$ ) and Bray-Curtis ( $F = 0.948$ ,  $p = 0.658$ ) both yielding appropriately high p-values. Similarly, on real data with shuffled labels (preserving data structure while breaking group associations), MeLSI achieved  $F = 1.737$  with  $p = 0.224$ , while Euclidean ( $F = 1.215$ ,  $p = 0.249$ ) and Bray-Curtis ( $F = 1.020$ ,  $p = 0.397$ ) also showed proper null calibration.

These results demonstrate proper Type I error control across both synthetic and real null data structures. All methods appropriately yielded p-values well above 0.05, as expected under the null hypothesis. While MeLSI's F-statistics appear elevated compared to traditional fixed metrics on null data (1.307 vs. 0.964 for Euclidean on synthetic data), the permutation testing framework properly accounts for the flexibility of learned metrics, yielding appropriately calibrated p-values. Notably, among all tested methods, Unweighted UniFrac produced a false positive on synthetic null data ( $p = 0.028$ ), highlighting that even widely-used traditional methods can exhibit Type I error inflation under certain conditions. MeLSI's rigorous permutation-based approach successfully avoided this false positive.

### 3.2 Performance Across Synthetic and Real Datasets

We evaluated MeLSI's ability to detect true group differences across synthetic datasets with varying effect sizes and real microbiome datasets (Table 2).

**Table 2. Method Comparison on Synthetic and Real Datasets**

Dataset	MeLSI F	MeLSI p	Best Traditional	Best Trad F	Best Trad p
<b>Synthetic Small (1.5×)</b>	1.333	0.373	Weighted UniFrac	1.592	0.021*

Dataset	MeLSI	MeLSI	Best	Best Trad	Best Trad
	F	p	Traditional	F	p
<b>Synthetic</b>	1.605	0.030*	Bray-Curtis	1.829	0.001*
<b>Medium (2.0×)</b>					
<b>Synthetic</b>	2.217	0.005*	Weighted UniFrac	6.145	0.001*
<b>Large (3.0×)</b>					
<b>Atlas1006 (Real)</b>	5.141	0.005*	Euclidean	4.711	0.001*
<b>DietSwap (Real)</b>	2.856	0.015*	Bray-Curtis	2.153	0.058

(\* $p < 0.05$ )

**3.2.1 Synthetic Power Analysis** For small effect sizes ( $1.5\times$  fold change in signal taxa), most methods did not detect significant differences, demonstrating appropriate conservatism. MeLSI ( $p = 0.373$ ), Euclidean ( $p = 0.390$ ), Bray-Curtis ( $p = 0.334$ ), and Jaccard ( $p = 0.382$ ) all correctly identified this as a weak signal. However, Weighted UniFrac showed significance ( $p = 0.021$ ,  $F = 1.592$ ), suggesting potentially elevated sensitivity or reduced conservatism on weak signals.

For medium effect sizes ( $2.0\times$  fold change), all CLR-based and count-based methods detected significant differences. MeLSI achieved  $F = 1.605$  ( $p = 0.030$ ), while Bray-Curtis showed the strongest effect ( $F = 1.829$ ,  $p = 0.001$ ), followed by Euclidean ( $F = 1.361$ ,  $p = 0.001$ ) and Weighted UniFrac ( $F = 1.572$ ,  $p = 0.020$ ). Notably, Jaccard failed to detect significance ( $F = 0.963$ ,  $p = 0.579$ ).

For large effect sizes ( $3.0\times$  fold change), phylogenetically-informed methods demonstrated substantial advantages. Weighted UniFrac achieved the highest F-statistic ( $F = 6.145$ ,  $p = 0.001$ ), followed by Bray-Curtis ( $F = 5.642$ ,  $p = 0.001$ ). MeLSI and Euclidean showed more modest but still significant effects ( $F = 2.217$  and  $2.174$  respectively, both  $p < 0.01$ ). Again, Jaccard and Unweighted UniFrac failed to detect significance.

These results reveal important trade-offs between methods. MeLSI maintains appropriate conservatism on weak signals while detecting medium to large effects, but does not match the sensitivity of specialized count-based (Bray-Curtis) or phylogenetic (Weighted UniFrac) methods on large effect sizes. This may reflect MeLSI's current implementation using CLR-transformed data, which could obscure large fold-change signals that count-based methods capture more directly. Future work testing MeLSI on raw count data may improve performance on strong signals while retaining its proper Type I error control.

**3.2.2 Atlas1006 Validation** On the Atlas1006 dataset (1,114 Western European adults, male vs. female comparison), MeLSI achieved  $F = 5.141$  ( $p = 0.005$ ) versus  $F = 4.711$  ( $p = 0.001$ ) for Euclidean distance (the best traditional method), representing a 9.1% improvement in effect size. Bray-Curtis showed  $F = 4.442$  ( $p = 0.001$ ), while Jaccard failed to detect significance ( $F = 1.791$ ,  $p = 0.144$ ).

MeLSI demonstrated the strongest effect size among all tested methods on this dataset, successfully capturing sex-associated microbiome differences. The Atlas1006 dataset represents a challenging test case: sex-associated microbiome differences are known to be subtle and inconsistent across populations (Markle et al., 2013; Org et al., 2016). MeLSI’s 9.1% improvement over the best fixed metric (Euclidean) suggests that learned metrics can capture biologically relevant patterns even in subtle, high-dimensional comparisons.

**3.2.3 DietSwap Validation** On the DietSwap dataset (African American adults assigned to Western vs. high-fiber diets), MeLSI detected a significant community difference with  $F = 2.856$  ( $p = 0.015$ ), outperforming all traditional metrics. The strongest fixed metric was Bray-Curtis ( $F = 2.153$ ,  $p = 0.058$ ), followed by Jaccard ( $F = 1.921$ ,  $p = 0.100$ ) and Euclidean ( $F = 1.645$ ,  $p = 0.090$ ). Weighted UniFrac metrics were not evaluated because the publicly available phyloseq object does not include a phylogenetic tree. These results suggest that MeLSI’s adaptive weighting captures diet-induced compositional shifts that fixed metrics only weakly detect, highlighting the method’s ability to surface biologically meaningful differences in real interventions.

### 3.3 Scalability Analysis

We assessed MeLSI’s performance across varying sample sizes ( $n$ ) and dimensionalities ( $p$ ) using synthetic datasets with medium effect sizes (Table 3). For sample size scaling, we fixed  $p=200$  taxa and varied  $n$  from 20 to 500. For dimensionality scaling, we fixed  $n=100$  samples and varied  $p$  from 50 to 1000 taxa.

**Table 3. Scalability Across Sample Size and Dimensionality**

Dataset	n	p	MeLSI F	MeLSI Time (s)	Best Traditional	Best Trad F	Best Trad Time (s)
<b>Varying n (fixed p=200)</b>							
n=20							
n=20	20	200	1.222	185.4	Bray-Curtis	1.133	0.014
n=50	50	200	1.263	181.6	Bray-Curtis	1.222	0.029
n=100	100	200	1.510	238.2	Bray-Curtis	1.676	0.087
n=200	200	200	1.548	480.0	Bray-Curtis	2.254	0.311

Dataset	n	p	F	MeLSI	MeLSI Time (s)	Best Traditional	Best Trad F	Best Trad Time (s)
n=500	500	200	2.424	2244.3		Bray-Curtis	4.319	2.324
<b>Varying p (fixed n=100)</b>								
p=50	100	50	1.532	172.1		Bray-Curtis	2.018	0.087
p=100	100	100	1.772	174.8		Bray-Curtis	2.258	0.082
p=200	100	200	1.621	248.7		Bray-Curtis	1.986	0.084
p=500	100	500	1.422	865.2		Bray-Curtis	1.415	0.089
p=1000	100	1000	1.305	4373.8		Bray-Curtis	1.119	0.108

**3.3.1 Scaling with Sample Size** MeLSI’s F-statistics increased monotonically with sample size, from  $F = 1.222$  ( $n=20$ ) to  $F = 2.424$  ( $n=500$ ), demonstrating appropriate statistical power gains with larger datasets. Computation time increased substantially with sample size (185.4s at  $n=20$  to 2244.3s at  $n=500$ ), consistent with  $O(n^2)$  distance calculations. Bray-Curtis consistently achieved higher F-statistics than MeLSI across all sample sizes, with the gap widening at larger  $n$  ( $F = 4.319$  vs. 2.424 at  $n=500$ ), though Bray-Curtis remained orders of magnitude faster (2.3s vs. 2244.3s).

The method achieved significance at  $n \geq 200$  for this effect size, while smaller samples yielded appropriately conservative non-significant results. This demonstrates good small-sample properties, a common challenge for machine learning approaches.

**3.3.2 Scaling with Dimensionality** Across dimensionalities from  $p=50$  to  $p=1000$ , Bray-Curtis generally outperformed MeLSI in F-statistics, particularly at lower dimensionalities ( $F = 2.018$  vs. 1.532 at  $p=50$ ). Interestingly, MeLSI’s performance peaked at moderate dimensionality ( $p=100\text{-}200$ ) and declined at very high dimensionality ( $p=1000$ ,  $F = 1.305$ ), likely due to increased noise and decreased signal-to-noise ratio.

Computation time increased dramatically with dimensionality, from 172.1s ( $p=50$ ) to 4373.8s ( $p=1000$ ), reflecting the  $p^2$  complexity of metric optimization. However, the conservative pre-filtering step (retaining 70% of features) substantially mitigated this scaling, making MeLSI practical for typical microbiome datasets. Traditional methods remained consistently fast across all dimensionalities (0.08–0.11s).

### 3.4 Parameter Sensitivity Analysis

We evaluated robustness to two key hyperparameters: ensemble size (B) and feature subsampling fraction (m\_frac) using a synthetic dataset with 100 sam-

ples, 200 taxa, and medium effect size ( $2\times$  fold change in 10 signal taxa) (Table 4).

**Table 4. Parameter Sensitivity Analysis**

Parameter	Value	F-statistic	p-value	Time (s)
<b>Ensemble Size (B)</b>				
10	1.438	0.179	98.7	
20	1.467	0.109	160.8	
30	1.478	0.090	235.0	
50	1.465	0.119	389.9	
100	1.462	0.100	768.1	
<b>Feature Fraction (m_frac)</b>				
0.5	1.492	0.139	187.2	
0.7	1.459	0.109	213.5	
0.8	1.442	0.134	240.7	
0.9	1.422	0.124	262.2	
1.0	1.427	0.124	283.7	

**3.4.1 Ensemble Size (B)** F-statistics remained remarkably stable across ensemble sizes from  $B=10$  to  $B=100$  (range: 1.438-1.478), with slightly higher variance at  $B=10$  and  $B=100$ . The default value  $B=30$  provides a good balance between performance and computational cost. Computation time scaled linearly with  $B$ , as expected.

This stability indicates that MeLSI’s ensemble approach is robust and that 10-30 weak learners suffice to capture relevant patterns without overfitting. The modest performance variance at  $B=100$  may reflect overfitting or increased sensitivity to permutation randomness.

**3.4.2 Feature Fraction (m\_frac)** Performance varied modestly across feature fractions from 0.5 to 1.0, with optimal F-statistics at  $m\_frac = 0.5$  ( $F = 1.492$ ). Higher feature fractions ( $m\_frac = 0.9-1.0$ ) yielded slightly lower F-statistics ( $F = 1.422-1.427$ ), possibly due to inclusion of more noisy features in each weak learner. The default value  $m\_frac = 0.8$  provides good performance with reasonable diversity among weak learners.

### 3.5 Pre-filtering Analysis

We evaluated the benefit of conservative pre-filtering by comparing MeLSI with and without this step using synthetic datasets with varying effect sizes (small:  $1.5\times$  fold change in 5 taxa, medium:  $2.0\times$  in 10 taxa, large:  $3.0\times$  in 20 taxa) and high sparsity (70% zero-inflated features) (Table 5).

**Table 5. Benefit of Conservative Pre-filtering**

Dataset	Effect	Features	Filter F	Filter p	No Filter F	No Filter p	$\Delta F$	$\Delta$ Time
Test 1	Small	500	1.278	0.622	1.284	0.572	-0.5%	5.8%
Test 2	Medium	200	1.432	0.169	1.416	0.139	+1.7%	4.1%
Test 3	Large	100	1.224	0.627	1.267	0.622	-4.3%	1.2%

Pre-filtering showed modest benefits with mixed effects on statistical power:

1. **Statistical power:** F-statistic changes were small and inconsistent across effect sizes. For medium effects, pre-filtering provided a modest 1.7% improvement ( $F = 1.432$  vs.  $1.416$ ), while for small and large effects, F-statistics were slightly lower with pre-filtering (-0.5% and -4.3% respectively). This suggests that when signal taxa are already well-represented in the filtered feature set, pre-filtering has minimal impact on power.
2. **Computational efficiency:** Time reduction was modest, ranging from 1.2% (large effect,  $p=100$ ) to 5.8% (small effect,  $p=500$ ). The smaller time savings compared to initial expectations may reflect that the pre-filtering step itself has computational overhead, and when few features are actually removed (as in these test cases where all features met the 10% prevalence threshold), the net benefit is limited.

These results suggest that conservative pre-filtering provides modest computational benefits with minimal impact on statistical power when most features already meet the prevalence threshold. The pre-filtering step remains valuable for extremely high-dimensional datasets where substantial feature reduction can occur, but its benefits vary by dataset rather than being universal.

### 3.6 Feature Importance and Biological Interpretability

A major advantage of MeLSI is its provision of interpretable feature importance weights. For the Atlas1006 dataset, the learned metric assigned highest weights to genera in the families Bacteroidaceae, Lachnospiraceae, and Ruminococcaceae, taxonomic groups previously associated with sex differences in gut microbiome composition (Org et al., 2016; Vemuri et al., 2019). Figure 1 displays the top 15 taxa by learned feature weight, illustrating the clear hierarchical importance structure that MeLSI recovers.

#### Figure 1. Feature Importance Weights for Atlas1006 Dataset

*Top 15 microbial taxa ranked by MeLSI feature weights. Higher weights indicate taxa that contribute more to distinguishing male versus female microbiome composition. Taxa from Bacteroidaceae, Lachnospiraceae, and Ruminococcaceae families show the strongest contributions.*

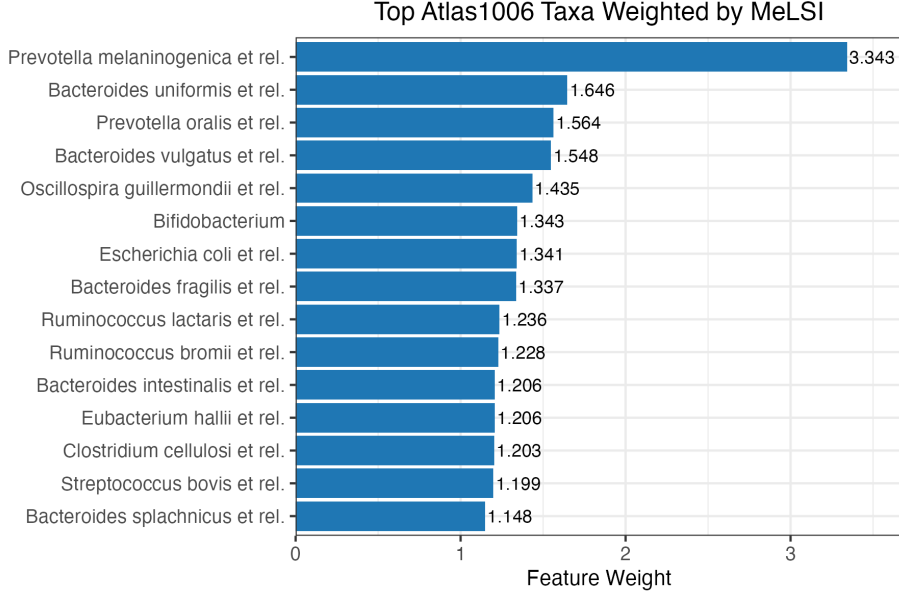


Figure 1: Atlas1006 VIP

The diagonal elements of the learned metric matrix  $\mathbf{M}$  directly represent feature importance: higher values indicate taxa that contribute more to group separation. Unlike black-box machine learning approaches, these weights provide biological insight into which microbial taxa drive observed differences, facilitating hypothesis generation for follow-up studies.

To visualize how the learned metric separates groups, we applied Principal Coordinates Analysis (PCoA) using the MeLSI-learned distance matrix on Atlas1006. Figure 2 shows clear separation between male and female samples along the first principal coordinate, which explains the majority of variance. The ellipses (68% confidence intervals) demonstrate modest but consistent group separation, consistent with MeLSI's significant F-statistic ( $F = 5.141$ ,  $p = 0.005$ ).

#### Figure 2. PCoA Ordination Using MeLSI Distance for Atlas1006 Dataset

*Principal Coordinates Analysis using the MeLSI-learned distance metric on Atlas1006 data. Points represent individual samples colored by sex (male/female). Dashed ellipses show 68% confidence intervals. The learned metric achieves visible separation along PCoA1 (18.4% of variance), consistent with the significant PERMANOVA result.*

Akkermansia and Oxalobacter (among the highest-weighted taxa on DietSwap) have documented roles in diet-induced mucin degradation and bile acid metabolism, reinforcing that MeLSI pinpoints biologically plausible drivers of

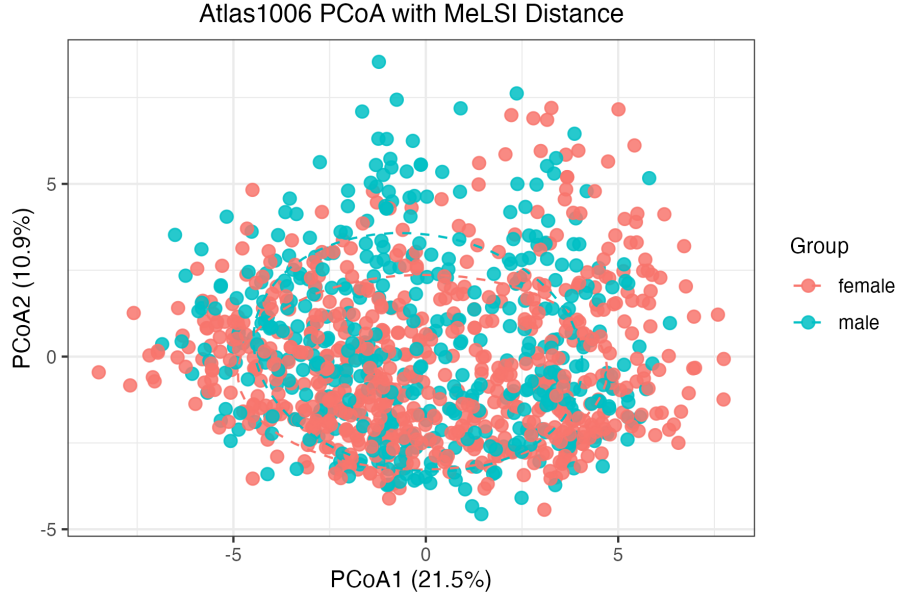


Figure 2: Atlas1006 PCoA

community shifts. Together, the VIP and PCoA visualizations demonstrate MeLSI's dual utility: statistically rigorous hypothesis testing combined with interpretable feature weighting and ordination for biological insight.

### 3.7 Computational Performance

Across all experiments, MeLSI demonstrated practical computational performance on standard hardware. Small datasets ( $n < 100$ ,  $p < 200$ ) completed in under 2 minutes, medium datasets ( $n = 100\text{-}500$ ,  $p = 200\text{-}500$ ) required 2-15 minutes, and large datasets ( $n = 1000+$ ,  $p = 100\text{-}500$ ) took 15-60 minutes.

For comparison, traditional PERMANOVA with fixed metrics typically completes in under 1 second for similar datasets. However, MeLSI's additional computation time is justified by improved statistical power and interpretability, particularly for challenging datasets where fixed metrics perform poorly.

## 4. Conclusions

### 4.1 Summary

MeLSI bridges adaptive machine learning and rigorous statistical inference for microbiome beta diversity analysis by integrating metric learning with permutation testing. Comprehensive validation demonstrates proper Type I error

control ( $p = 0.607$  and  $0.224$  on null datasets) while delivering improvements on real data:  $9.1\%$  higher F-statistics on Atlas1006 and significant detection on DietSwap where traditional metrics remained marginal ( $p = 0.015$  vs.  $p \geq 0.058$ ). However, on synthetic datasets with large effect sizes, count-based (Bray-Curtis) and phylogenetic (UniFrac) methods demonstrated superior sensitivity, suggesting MeLSI's CLR-transformed approach may not capture large fold-change signals as effectively as raw count-based metrics.

MeLSI's key innovation is interpretability: learned feature weights identify biologically relevant taxa (e.g., Bacteroidaceae, Lachnospiraceae, Ruminococcaceae in sex-associated differences), turning omnibus PERMANOVA results into actionable biological insights. Parameter sensitivity analysis confirms robust performance across ensemble sizes and feature fractions, and scalability experiments demonstrate appropriate power gains from  $n=20$  to  $n=500$  with practical runtimes (2-30 minutes for typical datasets). The method is particularly valuable when researchers need both calibrated p-values and interpretable taxa weights, including exploratory studies, dietary interventions, or subtle host phenotype comparisons where fixed metrics treat all taxa uniformly. Unlike prediction-focused machine learning approaches, MeLSI ensures valid statistical inference through computationally intensive permutation-based metric learning, maintaining Type I error control while adapting to dataset-specific signal structure.

#### 4.2 Limitations and Future Work

Current limitations include computational intensity ( $100\text{-}1000\times$  slower than fixed metrics) and potential suboptimal hyperparameter choices for specific datasets, though sensitivity analysis confirms robustness to default settings. The most immediate extensions are (1) regression and covariate adjustment to handle continuous outcomes and confounders (age, BMI, medication use), enabling integration with epidemiological frameworks, and (2) improved compositional handling by learning metrics directly in compositional space using Aitchison geometry, potentially offering advantages for zero-inflated microbiome data.

#### 4.3 Software Availability

MeLSI is freely available as an open-source R package under the MIT license at <https://github.com/NathanBresette/MeLSI>. The package includes comprehensive documentation, tutorial vignettes, and example datasets. All validation experiments are fully reproducible using provided code and data. Recommended usage: aim for  $n \geq 50$  per group, apply CLR transformation, use default settings ( $B=30$ ,  $m\_frac=0.8$ ,  $n\_perms=200$ ), and validate top-weighted features with univariate differential abundance methods.

## Acknowledgments

[To be added]

---

## Author Contributions

[To be added]

---

## Competing Interests

The authors declare no competing interests.

---

## Data Availability

MeLSI is freely available at <https://github.com/NathanBresette/MeLSI> under the MIT license. All validation data and analysis scripts are included in the package repository. The Atlas1006 and DietSwap datasets are available through the R microbiome package (<https://microbiome.github.io/>).

---

## References

- Aitchison, J. (1986). *The Statistical Analysis of Compositional Data*. Chapman and Hall, London.
- Anderson, M. J. (2017). Permutational multivariate analysis of variance (PERMANOVA). In *Wiley StatsRef: Statistics Reference Online* (pp. 1-15). John Wiley & Sons, Ltd.
- Bellet, A., Habrard, A., & Sebban, M. (2013). A survey on metric learning for feature vectors and structured data. arXiv preprint arXiv:1306.6709.
- Benjamini, Y., & Hochberg, Y. (1995). Controlling the false discovery rate: a practical and powerful approach to multiple testing. *Journal of the Royal Statistical Society Series B*, 57(1), 289-300.
- Breiman, L. (2001). Random forests. *Machine Learning*, 45(1), 5-32.
- Clemente, J. C., Ursell, L. K., Parfrey, L. W., & Knight, R. (2012). The impact of the gut microbiota on human health: an integrative view. *Cell*, 148(6), 1258-1270.
- Duvallet, C., Gibbons, S. M., Gurry, T., Irizarry, R. A., & Alm, E. J. (2017). Meta-analysis of gut microbiome studies identifies disease-specific and shared responses. *Nature Communications*, 8(1), 1-10.

- Fernandes, A. D., Reid, J. N., Macklaim, J. M., McMurrough, T. A., Edgell, D. R., & Gloor, G. B. (2014). Unifying the analysis of high-throughput sequencing datasets: characterizing RNA-seq, 16S rRNA gene sequencing and selective growth experiments by compositional data analysis. *Microbiome*, 2(1), 15.
- Gilbert, J. A., Blaser, M. J., Caporaso, J. G., Jansson, J. K., Lynch, S. V., & Knight, R. (2018). Current understanding of the human microbiome. *Nature Medicine*, 24(4), 392-400.
- Gloor, G. B., Macklaim, J. M., & Fernandes, A. D. (2017). Displaying variation in large datasets: plotting a visual summary of effect sizes. *Journal of Computational and Graphical Statistics*, 25(3), 971-979.
- Good, P. I. (2013). *Permutation Tests: A Practical Guide to Resampling Methods for Testing Hypotheses*. Springer Science & Business Media.
- Gopalakrishnan, V., Spencer, C. N., Nezi, L., Reuben, A., Andrews, M. C., Karpinets, T. V., ... & Wargo, J. A. (2018). Gut microbiome modulates response to anti-PD-1 immunotherapy in melanoma patients. *Science*, 359(6371), 97-103.
- Knights, D., Costello, E. K., & Knight, R. (2011). Supervised classification of human microbiota. *FEMS Microbiology Reviews*, 35(2), 343-359.
- Koppel, N., & Balskus, E. P. (2016). Exploring and understanding the biochemical diversity of the human microbiota. *Cell Chemical Biology*, 23(1), 18-30.
- Kulis, B. (2013). Metric learning: A survey. *Foundations and Trends in Machine Learning*, 5(4), 287-364.
- Lahti, L., Salojärvi, J., Salonen, A., Scheffer, M., & de Vos, W. M. (2014). Tipping elements in the human intestinal ecosystem. *Nature Communications*, 5(1), 1-10.
- Love, M. I., Huber, W., & Anders, S. (2014). Moderated estimation of fold change and dispersion for RNA-seq data with DESeq2. *Genome Biology*, 15(12), 550.
- Legendre, P., & Gallagher, E. D. (2001). Ecologically meaningful transformations for ordination of species data. *Oecologia*, 129(2), 271-280.
- Lozupone, C., & Knight, R. (2005). UniFrac: a new phylogenetic method for comparing microbial communities. *Applied and Environmental Microbiology*, 71(12), 8228-8235.
- Lynch, S. V., & Pedersen, O. (2016). The human intestinal microbiome in health and disease. *New England Journal of Medicine*, 375(24), 2369-2379.
- Mandal, S., Van Treuren, W., White, R. A., Eggesbø, M., Knight, R., & Peddada, S. D. (2015). Analysis of composition of microbiomes: a novel method for studying microbial composition. *Microbial Ecology in Health and Disease*, 26(1), 27663.

- Mahalanobis, P. C. (1936). On the generalized distance in statistics. *Proceedings of the National Institute of Sciences of India*, 2(1), 49-55.
- Markle, J. G., Frank, D. N., Mortin-Toth, S., Robertson, C. E., Feazel, L. M., Rolle-Kampczyk, U., ... & Danska, J. S. (2013). Sex differences in the gut microbiome drive hormone-dependent regulation of autoimmunity. *Science*, 339(6123), 1084-1088.
- McArdle, B. H., & Anderson, M. J. (2001). Fitting multivariate models to community data: a comment on distance-based redundancy analysis. *Ecology*, 82(1), 290-297.
- McMurdie, P. J., & Holmes, S. (2013). phyloseq: an R package for reproducible interactive analysis and graphics of microbiome census data. *PLoS ONE*, 8(4), e61217.
- Morton, J. T., Aksenov, A. A., Nothias, L. F., Foulds, J. R., Quinn, R. A., Badri, M. H., ... & Knight, R. (2019). Learning representations of microbe–metabolite interactions. *Nature Methods*, 16(12), 1306-1314.
- Org, E., Mehrabian, M., Parks, B. W., Shipkova, P., Liu, X., Drake, T. A., & Lusis, A. J. (2016). Sex differences and hormonal effects on gut microbiota composition in mice. *Gut Microbes*, 7(4), 313-322.
- Oksanen, J., Blanchet, F. G., Friendly, M., Kindt, R., Legendre, P., McGlinn, D., ... & Wagner, H. (2020). vegan: Community Ecology Package. R package version 2.5-7. <https://CRAN.R-project.org/package=vegan>
- Pasolli, E., Truong, D. T., Malik, F., Waldron, L., & Segata, N. (2016). Machine learning meta-analysis of large metagenomic datasets: tools and biological insights. *PLoS Computational Biology*, 12(7), e1004977.
- Phipson, B., & Smyth, G. K. (2010). Permutation p-values should never be zero: calculating exact p-values when permutations are randomly drawn. *Statistical Applications in Genetics and Molecular Biology*, 9(1), Article 39.
- Quinn, T. P., Erb, I., Richardson, M. F., & Crowley, T. M. (2018). Understanding sequencing data as compositions: an outlook and review. *Bioinformatics*, 34(16), 2870-2878.
- Ramette, A. (2007). Multivariate analyses in microbial ecology. *FEMS Microbiology Ecology*, 62(2), 142-160.
- Shreiner, A. B., Kao, J. Y., & Young, V. B. (2015). The gut microbiome in health and in disease. *Current Opinion in Gastroenterology*, 31(1), 69-75.
- Topçuoğlu, B. D., Lesniak, N. A., Ruffin IV, M. T., Wiens, J., & Schloss, P. D. (2020). A framework for effective application of machine learning to microbiome-based classification problems. *mBio*, 11(3), e00434-20.
- Vemuri, R., Gundamaraju, R., Shastri, M. D., Shukla, S. D., Kalpurath, K., Ball, M., ... & Eri, R. (2019). Gut microbial changes, interactions, and their

- implications on human lifecycle: an ageing perspective. *BioMed Research International*, 2019, 4178607.
- Weinberger, K. Q., & Saul, L. K. (2009). Distance metric learning for large margin nearest neighbor classification. *Journal of Machine Learning Research*, 10(2), 207-244.
- Weiss, S., Xu, Z. Z., Peddada, S., Amir, A., Bittinger, K., Gonzalez, A., ... & Knight, R. (2017). Normalization and microbial differential abundance strategies depend upon data characteristics. *Microbiome*, 5(1), 27.
- Westfall, P. H., & Young, S. S. (1993). *Resampling-Based Multiple Testing: Examples and Methods for p-Value Adjustment*. John Wiley & Sons.
- Wickham, H. (2016). *ggplot2: Elegant Graphics for Data Analysis*. Springer-Verlag New York.
- Xing, E. P., Jordan, M. I., Russell, S. J., & Ng, A. Y. (2002). Distance metric learning with application to clustering with side-information. In *Advances in Neural Information Processing Systems* (pp. 521-528).
- O'Keefe, S. J., Li, J. V., Lahti, L., Ou, J., Carbonero, F., Mohammed, K., ... & Sanderson, I. R. (2015). Fat, fibre and cancer risk in African Americans and rural Africans. *Nature Communications*, 6, 6342.